

# Blumlein Configuration for High-Repetition-Rate Pulse Generation of Variable Duration and Polarity Using Synchronized Switch Control

Matej Reberšek, Matej Kranjc, Denis Pavliha, Tina Batista-Napotnik, Danilo Vrtačnik, Slavko Amon, *Member, IEEE*, and Damijan Miklavčič\*

**Abstract**—Blumlein generators are used in different applications such as radars, lasers, and also recently in various biomedical studies, where the effects of high-voltage nanosecond pulses on biological cells are evaluated. In these studies, it was demonstrated that by applying high-voltage nanosecond pulses to cells, plasma membrane and cell organelles are permeabilized. As suggested in a recent publication, the repetition rate and polarity of nanosecond high-voltage pulses could have an important effect on the electroporation process, and consequently, on the observed phenomena. Therefore, we designed a new Blumlein configuration that enables a higher repetition rate of variable duration of either bipolar or unipolar high-voltage pulses. We achieved a maximal pulse repetition rate of 1.1 MHz. However, theoretically, this rate could be even higher. We labeled endocytotic vesicles with lucifer yellow and added propidium iodide to a cell suspension for testing the cell plasma membrane integrity, so we were able to observe the permeabilization of endocytotic vesicles and the cell plasma membrane at the same time. The new design of pulse generator was built, verified, and also tested in experiments. The resulting flexibility and variability allow further *in vitro* experiments to determine the importance of the pulse repetition rate and pulse polarity on membrane permeabilization—both of the cell plasma membrane as well as of cell organelle membranes.

**Index Terms**—Blumlein generator, electroporation, endocytotic vesicles, high repetition rate.

## I. INTRODUCTION

**E**LECTROPORATION is a phenomenon in which increased cell membrane permeability is observed after the cell membrane is exposed to a sufficiently high electric field. This phenomenon is now used in oncology, genetics, and cell biology for the internalization of a wide range of substances and also for the fusion of cells [1]–[3]. The electric field for electroporation is generated by means of a device—an electroporator delivering electric pulses [4]. Most commonly used electroporators generate electric pulses in the range of a few

microseconds up to several milliseconds. Recently, a new type of electroporators named nanoporators was developed and used in biology, generating electric pulses of only a few nanoseconds duration [5], [6].

The design of a nanoporator is usually based on a Blumlein generator. The Blumlein generator is a pulse generator based on a pulse forming network [7]. The most basic configuration of a Blumlein generator consists of a transmission line connected to a high-voltage source via a high-impedance resistor. After the transmission line accumulates electric energy, it is discharged into the load by a high-voltage switch [8]. Blumlein generators operated by very fast switches are adequate for generating pulses having a short rise time, and consequently, for generating pulses of short duration. The duration of the pulse generated by means of a basic Blumlein generator depends on the length of the transmission line only and is, therefore, of a fixed duration [5], [6].

Blumlein generators are used in different applications such as radars [9] and lasers [10]. Recently, Blumlein generators have also been used in various biomedical studies, where the effects of high-voltage nanosecond pulses on biological cells were evaluated and have been suggested to reach into the cell interior without affecting the cell plasma membrane [11]–[13]. Large endocytic vacuoles were selectively permeabilized with little effect on the integrity of the outer cell membrane [14]. However, recent studies show that by applying high-voltage nanosecond pulses, the cell plasma membrane is also permeabilized [15], [16]. Researchers have demonstrated that nanosecond pulsed electric fields can induce apoptosis and inhibit tumor growth [17], [18] and so may be further developed as a possible treatment for basal cell carcinoma [19].

Different pulse parameters have different effects on cells and, as has been recently suggested [20], the repetition rate and polarity of nanosecond high-voltage pulses could have an important effect on the electroporation process, and consequently, on the observed phenomena. However, the maximal repetition rate of nanoporators is limited by the charging time and, according to previous publications, is limited to 10 kHz [20]. We, therefore, suggest a new Blumlein configuration that enables a higher repetition rate of variable duration of either bipolar or unipolar high-voltage pulses by further developing a recently suggested Blumlein configuration for a variable duration of the high-voltage pulse [21], [22].

Our aim in this study was to develop and test a new device for the electroporation of cells and their organelles with variable length and polarity and high repetition frequency of

Manuscript received February 25, 2009; revised May 1, 2009 and June 12, 2009. First published July 24, 2009; current version published October 16, 2009. This work was supported by the Slovenian Research Agency (ARRS) under Grant Z2-7046 and Grant P2-0249. Asterisk indicates corresponding author.

M. Reberšek, M. Kranjc, D. Pavliha, T. Batista-Napotnik, D. Vrtačnik, and S. Amon are with the Faculty of Electrical Engineering, University of Ljubljana, Ljubljana SI-1000, Slovenia (e-mail: matej.rebersek@fe.uni-lj.si; matej.kranjc@fe.uni-lj.si; denis.pavliha@fe.uni-lj.si; tina.batistanaapotnik@fe.uni-lj.si; danilo.vrtacnik@fe.uni-lj.si; slavko.amon@fe.uni-lj.si).

\*D. Miklavčič is with the Faculty of Electrical Engineering, University of Ljubljana, Ljubljana SI-1000, Slovenia (e-mail: damijan.miklavcic@fe.uni-lj.si).

Digital Object Identifier 10.1109/TBME.2009.2027422

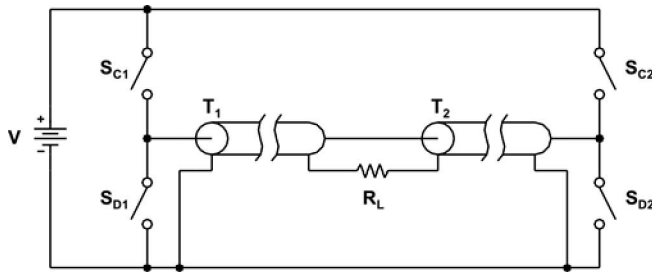


Fig. 1. Conceptual schematic of suggested Blumlein configuration for high-repetition-rate pulse generation of variable duration and polarity.  $S_{C1}$  and  $S_{C2}$  are charging switches and  $S_{D1}$  and  $S_{D2}$  are discharging switches for  $T_1$  and  $T_2$  transmission lines.  $V$  is a power supply of the generator and  $R_L$  the resistance of the load.

high-voltage nanosecond pulses. For this purpose, we developed a new charge and discharge unit and a new delay unit for the Blumlein generator. The use of the generator was also tested on cultured cells: we applied high-voltage nanosecond pulses to a B16 F1 mouse melanoma cell line and achieved a permeabilization of both the cell plasma membrane and the endocytotic vesicles.

## II. MATERIALS AND METHODS

### A. Functional Description of the Suggested Blumlein Configuration

In the basic Blumlein configuration, each pulse generated has to be delayed for as long as the transmission line passively charges through the high-impedance resistor. In our newly developed configuration (Fig. 1) under ideal conditions, each pulse can be generated immediately after another. Suppose that the equivalent transmission lines  $T_1$  and  $T_2$  are discharged. In practice, this can be achieved by using a high-impedance resistor. At this moment, we start charging transmission lines  $T_1$  and  $T_2$  simultaneously over charging switches  $S_{C1}$  and  $S_{C2}$ . After time  $\tau$ , the transmission lines are charged but no pulse is generated on load  $R_L$ . Time  $\tau$  equals the electrical length or propagation delay of each transmission line. However, if the turn-ON time of charging switch  $S_{C2}$  is shifted by  $\Delta T_1 \neq 0$ , a square pulse is generated on the load  $R_L$  (Fig. 2). The duration of the pulse equals  $\Delta T_1$  if  $|\Delta T_1| < 2\tau$ ; otherwise, the duration of the pulse equals  $2\tau$ . The polarity of the pulse depends on which switch  $S_{C1}$  or  $S_{C2}$  is turned on first. With the described sequences of switching, we can, therefore, charge the transmission lines or also generate a high-voltage pulse of variable duration and polarity. After charging the transmission lines  $T_1$  and  $T_2$ , charging switches  $S_{C1}$  and  $S_{C2}$  can be turned off and discharging switches  $S_{D1}$  and  $S_{D2}$  can be turned on. Under ideal conditions, the charging time of transmission lines  $T_1$  and  $T_2$  varies from  $\tau$  to  $2\tau$  and depends on  $\Delta T_1$ . From this point on discharging the transmission lines  $T_1$  and  $T_2$  and generating the second pulse, the first or none is almost the same as in the first sequence, as shown in Fig. 2 and was also described previously [21]. The maximal repetition rate of pulse generation can therefore be in the range from  $1/2\tau$  to  $1/\tau$ .

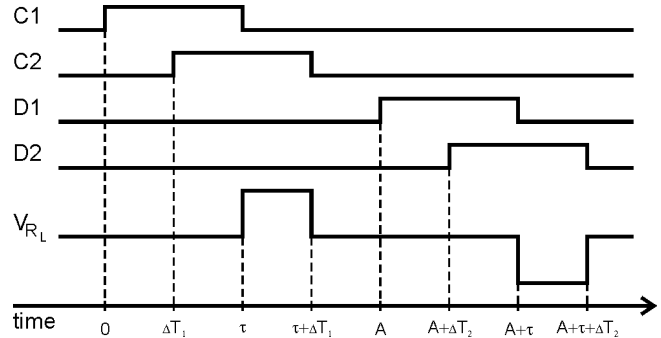


Fig. 2. Time diagram of suggested configuration of pulse generation for high-repetition-rate pulse generation.  $C1$ ,  $C2$ ,  $D1$ , and  $D2$  are ON/OFF (respectively high/low) signals for switches  $S_{C1}$ ,  $S_{C2}$ ,  $S_{D1}$ , and  $S_{D2}$  (Fig. 1).  $V_{R_L}$  is the voltage on the load.  $\Delta T_1$  and  $\Delta T_2$  are delays between turn-ON time of charge and discharge switches, respectively. Time  $\tau$  equals electrical length or propagation delay of transmission lines  $T_1$  and  $T_2$ . Time  $A$  is a repetition time of the pulses.

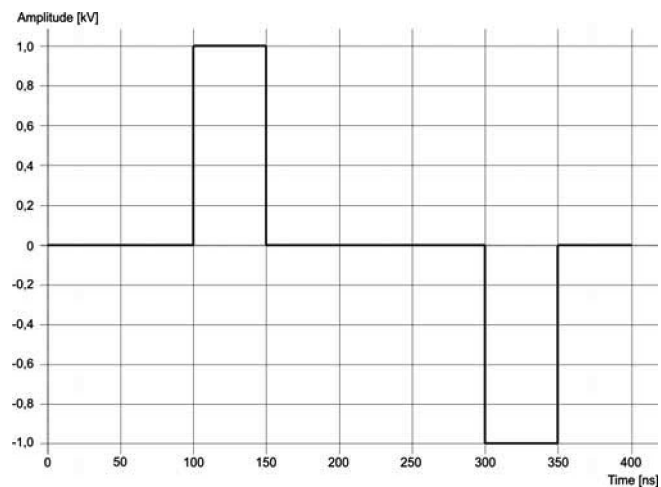


Fig. 3. Output voltage of suggested Blumlein configuration as a result of SPICE simulation under ideal conditions. Result shows high-repetition-rate bipolar nanosecond pulses.

### B. Simulation of the Suggested Blumlein Configuration

To verify the suggested configuration of pulse generation, we first simulated the suggested Blumlein configuration (Fig. 1) using the SPICE OPUS circuit simulator (CACD group, Slovenia). In this simulation, all circuit elements were considered to be ideal. For the simulation, we used a 1-kV dc voltage supply  $V$  and a 100- $\Omega$  load  $R_L$  placed between transmission lines  $T_1$  and  $T_2$ . Each transmission line had a delay  $\tau$  of 100 ns and characteristic impedance  $Z_0$  of 50  $\Omega$ . The simulation was performed with transient analysis at a time step of 10 ps and a simulation time of 400 ns. Switches ( $S_{C1}$ ,  $S_{C2}$ ,  $S_{D1}$ , and  $S_{D2}$ ) were driven with simulated digital pulses, as depicted in Fig. 2, with a 100 ns duration of each single pulse. The delay  $\Delta T_1$  between turn-ON time of  $S_{C1}$  and  $S_{C2}$  and the delay  $\Delta T_2$  between turn-ON time of  $S_{D1}$  and  $S_{D2}$  were 50 ns. The turn-ON time of  $S_{D1}$  was delayed for  $A = 200$  ns with respect to the turn-ON time of  $S_{C1}$ . The simulation result is presented in Fig. 3.

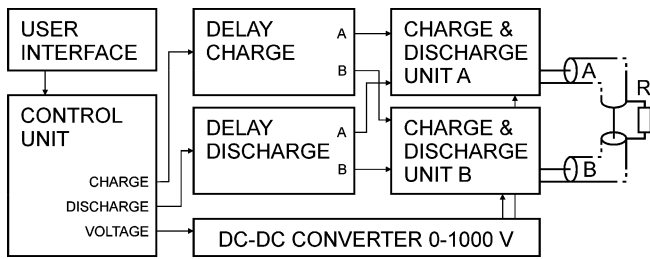


Fig. 4. Block diagram of new device setup. User interface allows entering electric parameters of the nanosecond pulses. Control unit controls two delay units and high-voltage power supply and generates charge and discharge pulses. Delay units delay charge and discharge pulses to achieve desired delays  $T_1$  and  $T_2$ . Charge and discharge units are made up of two RF Switch Mode MOSFETs to charge and discharge transmission lines A and B.  $R$  is the resistance of the load.

### C. Device Setup

The new device consists of a user interface, control unit, high-voltage power supply, two delay units, and two charge and discharge units (Fig. 4). The user interface was developed on the Mini-ITX platform (EPIA-EN12000EG, VIA, China) with a touch screen (1537L, EloTouch, USA). The application was programmed in Visual Basic .NET (Visual Studio 2005, Microsoft, USA) and it is hosted on Compact Framework 2.0 on a custom-built operation system (Windows CE .NET, Microsoft, USA). The user interface allows the entering of the electric parameters of the nanosecond pulses into the device: voltage, duration, number of pulses, and frequency of pulses. The control unit is connected to the Mini-ITX platform by USB2.0 and was developed on FPGA (XC3S200, Xilinx, USA). The control unit controls the high-voltage power supply and two delay units and also generates charge and discharge pulses. The high-voltage power supply consists of a 100 W half bridge dc-to-dc converter and a 0.1 A constant current discharger so that any voltage can be obtained in less than 500 ms. The output voltage of the power supply can be set from 250 to 1000 V. The delay units are made of an analog multiplier (AD835, Analog Devices, USA), an integrator, and a Schmitt trigger [AD8099, Analog Devices, USA; Fig. 5(a)]. The analog multiplier multiplies digital pulse ( $U_P$ ) with voltage ( $U_V$ ) defined by the control unit. The output signal of the multiplier ( $U_M$ ) is then integrated ( $U_I$ ) and send through the Schmitt trigger ( $U_O$ ). Taking into account the input pulse ( $U_P$ ), the delay of output pulse ( $U_O$ ) depends on amplitude of  $U_V$ . Digital pulses can thus by our delay unit be delayed ( $\Delta T$ ) from 20 to 300 ns with  $\pm 10\%$  ( $\pm 2$ –30 ns) accuracy [Fig. 5(b)] to achieve the desired delays  $\Delta T_1$  and  $\Delta T_2$  (Fig. 2). The charge and discharge units are made of two RF Switch Mode MOSFETs (DE275-102N06A, Ixys, USA). The MOSFET's rise times are delayed to 16 ns in order to reduce electromagnetic interference with low-voltage circuits.

### D. Electrode Chamber

An electrode chamber was built consisting of electrodes on cover glass, an electrode holder for a microscope, and two transmission lines. The electrode structure (Fig. 6) was fabricated directly on a 25 mm  $\times$  40 mm cover glass (BB025040A1#1,

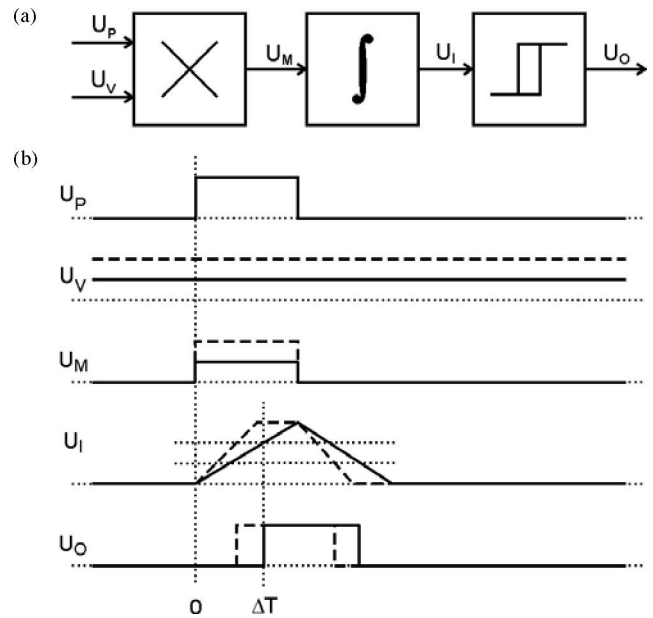


Fig. 5. Block diagram of (a) delay unit and (b) time diagram of delay unit signals. The delay unit is made up of an analog multiplier, an integrator, and a Schmitt trigger.  $U_P$  is a digital input pulse that is delayed by the delay unit.  $U_V$  is a voltage constant inversely proportional to delay time  $\Delta T$ .  $U_M$  is an output signal of the multiplier,  $U_I$  is an output signal of the integrator, and  $U_O$  is an output signal of the Schmitt trigger. Continuous lines represent the signals (b). Dashed lines represent signals at higher voltage constant  $U_V$ . Dotted lines are assisting time and voltage lines. At signal  $U_I$ , there are two assisting voltage lines for Schmitt-trigger hysteresis.

Menzel-Gläser, Germany), using conventional microelectromechanical systems (MEMS) techniques. The first step in electrode fabrication was the wet chemical cleaning of substrate in SC1 solution (1:1:5  $\text{NH}_3\text{OH}:\text{H}_2\text{O}_2:\text{H}_2\text{O}$  at 75 °C) followed by sputter deposition of a Cr/Au metal sandwich with thicknesses 10 nm/100 nm, respectively. A thin Cr film was used to enhance the adhesion of the gold layer to the substrate. The second step was the standard photolithographic patterning of negative tone photoresist AZ nLOF 2035 (Clariant, USA) with thickness 6  $\mu\text{m}$ . A patterned photoresist was hardened at a temperature of 150 °C, with the aim of improving the adhesion of the photoresist to the sputtered gold layer and increasing the resistance of the photoresist to wet etching and to the deposition of electroplated gold in subsequent steps [Fig. 6(a)].

The electroplating of gold was performed in a standard gold-cyanide solution for the deposition of thin electroplating layers with a deposition rate of 5  $\mu\text{m}/\text{h}$ , thus resulting in a 6- $\mu\text{m}$ -thick gold layer. A dc current source providing a current density of 100  $\text{mA}/\text{cm}^2$  was applied during the electroplating deposition. After the electroplating of gold, the resist was removed in an ultrasonic bath by N-methyl-2-pyrrolidone (NMP) at 60 °C for 1 h. In the final step, the sputtered metal sandwich was removed by wet chemical etching. Gold was etched in a mixture of  $\text{HNO}_3 : \text{HCl} : \text{DI}$  (1:1:4) at the etching rate of 30 nm/min. The chrome layer was etched by the commercial chromium etchant CR-14 from Cynatek Corporation, USA, for 10 s. After etching, the sample was rinsed in deionized (DI) water and blown with dry nitrogen [Fig. 6(b)]. The final gold electrodes thickness and the width of the air gap between the two electrodes are typically

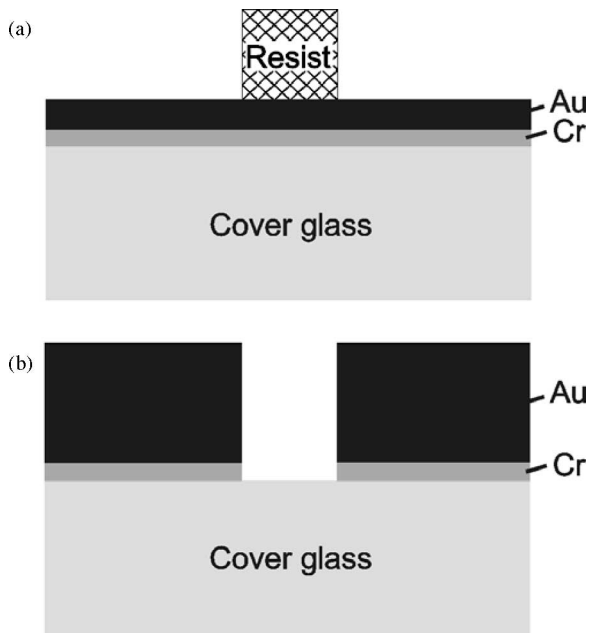


Fig. 6. Schematic presentation of electrode structure fabrication after (a) Cr/Au metal deposition and resist photolithography and (b) final steps, i.e. deposition of electroplated gold, resist removing and wet etching of sputter deposited Cr/Au layers.

5.0 and 100  $\mu\text{m}$ , respectively. Accurate structure dimensions were determined by measurement with Talysurf Stylus Profiler.

The electrodes on the cover glass were glued and soldered to the holder. The transmission lines made by coaxial cable RG174A/U ( $2 \times 25$  m, 100 pF/m, 50  $\Omega$ ; Nexans, France) and an impedance matching resistor were also soldered to the holder.

### E. Cells and Labeling

B16 F1 mouse melanoma cells (ATCC, USA) were cultured in Eagle's minimal essential medium (EMEM) culture medium with L-glutamine (Sigma–Aldrich, USA) supplemented with 10% fetal bovine serum (FBS) and antibiotics, seeded in six-well plates, one or two days before experiments, at the concentration of  $10^4$  or  $5 \times 10^3$  cells/cm<sup>2</sup>, respectively. They were first loaded with 1 mM lucifer yellow (Sigma–Aldrich, USA) [23] in a porating phosphate buffer, which consisted of 250 nM sucrose, 10 mM phosphate ( $\text{K}_2\text{HPO}_4/\text{KH}_2\text{PO}_4$ ) and 1 mM  $\text{MgCl}_2$ , pH 7.4, and electrical conductivity 1.67 mS/cm [24], [25]. The cells were then incubated for 2 h at 37  $^\circ\text{C}$  in a  $\text{CO}_2$  incubator and afterwards washed three times with EMEM culture medium, trypsinized, centrifuged in EMEM (1000 r/min, 5 min, 4  $^\circ\text{C}$ ), and resuspended in porating phosphate buffer in a concentration of  $10^6$  cells/mL. To 20  $\mu\text{L}$  of cell suspension, 100  $\mu\text{g}/\text{mL}$  propidium iodide (Sigma–Aldrich, USA) was added just before exposure to electric pulses [26]. The cells were put between the electrodes and observed under a fluorescent microscope (Zeiss, Göttingen, Germany), using a 40 $\times$  objective. The cells were exposed to 20 electric pulses of 60 ns duration, 50 kV/cm field strength, and pulse repetition frequency of 1 kHz. Phase contrast and fluorescent images were taken before and 10 min after pulsing. For observing lucifer yellow,  $\lambda_{\text{ex}}$  was 425 nm and  $\lambda_{\text{em}}$

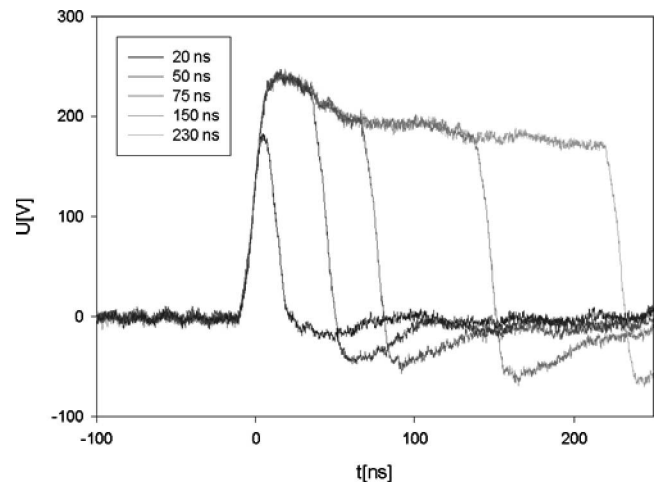


Fig. 7. Nanosecond pulses with various durations (20, 50, 75, 150, and 230 ns) generated by the new device. Pulses are generated on a 100- $\Omega$  resistor and measured by oscilloscope (WavePro 7300A, LeCroy, USA) using a high-voltage probe (PPE2KV, LeCroy, USA).

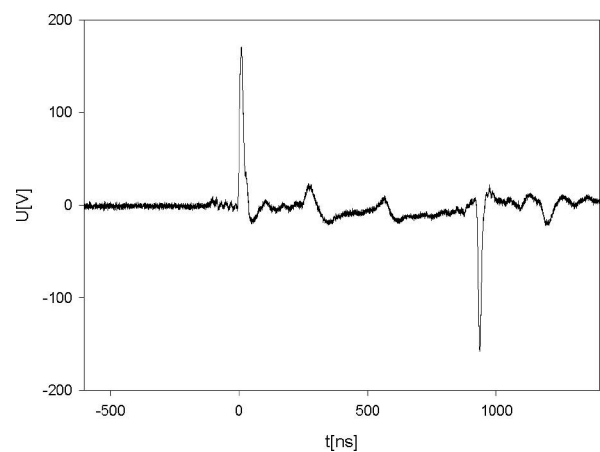


Fig. 8. High-repetition-rate (1.1 MHz) bipolar nanosecond pulses generated by the new device. Pulses are generated on a 100- $\Omega$  resistor and measured by oscilloscope (WavePro 7300A, LeCroy, USA) using a high-voltage probe (PPE2KV, LeCroy, USA).

was 510 nm, and for propidium iodide,  $\lambda_{\text{ex}}$  was 540 nm and  $\lambda_{\text{em}}$  was 640 nm.

## III. RESULTS

### A. Device Performance

Two tests were made with the newly developed Blumlein configuration. One was made to test variable duration (Fig. 7), and the other one to test the high repetition rate and the bipolarity (Fig. 8) of the nanosecond pulses generated. In the first test,  $S_{C1}$  and  $S_{C2}$  were turned on with different delays  $\Delta T_1$ , so that nanosecond pulses with various duration (20, 50, 75, 150, and 230 ns, Fig. 7) were generated. In the second test, the delays  $\Delta T_1$  and  $\Delta T_2$  were 20 ns and delay  $A$  was 910 ns. As a result, we generated two nanosecond pulses on  $R_L$  with high repetition rate and of opposite polarity (Fig. 8). All electric measurements

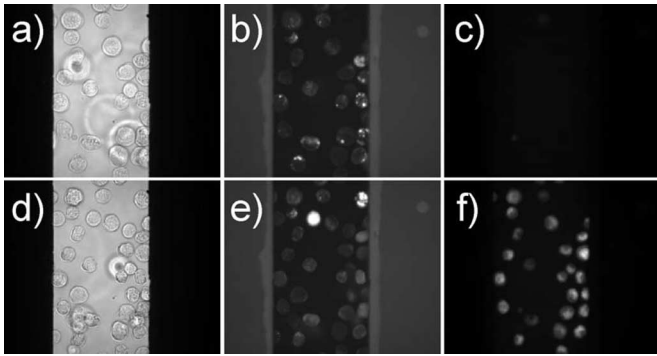


Fig. 9. B16 F1 mouse melanoma cells (a)–(c) before exposing and (d)–(f) after exposure to 20 electric pulses (duration 60 ns, field strength 50 kV/cm, repetition rate 1 kHz). (a) and (d) Phase contrast. (b) and (e) Lucifer yellow (labeling of endocytotic vesicles). (c) and (f) Propidium iodide (enters the cell if the cell plasma membrane is permeabilized). After exposing cells to electric pulses, the endocytotic vesicles released lucifer yellow into the cytoplasm (in (e), the vesicles are less visible, and the whole cell is labeled with the dye). Propidium iodide entered the cell after cell exposure to electric pulses (f).

were done by oscilloscope (WavePro 7300A, LeCroy, USA) and a high-voltage probe (PPE2KV, LeCroy, USA).

### B. Permeabilization of Cellular Membranes

Labeled cells B16 F1 were placed between the electrodes [Fig. 9(a)] and were observed under a microscope (40 $\times$  objective). Endocytotic vesicles in B16 F1 mouse melanoma cells are visible before pulsing due to loading with lucifer yellow [Fig. 9(b)]. Cells in control not exposed to electric pulses excluded propidium iodide [Fig. 9(c)]. After the cells were exposed to electrical pulses, the endocytotic vesicles released lucifer yellow into the cytoplasm—after 10 min, the vesicles were less visible and the whole cytoplasm was labeled by the dye [Fig. 9(e)]. At the same time, the cell plasma membrane was also permeabilized—which is indicated by propidium iodide entering the cells and labeling the DNA within the cells [Fig. 9(f)].

In sham-exposed cells, there was no lucifer yellow release from endocytotic vesicles and no propidium iodide entering cells (data not shown).

## IV. DISCUSSION AND CONCLUSION

In this paper, we present a modified Blumlein configuration for high-repetition-rate pulse generation. Pulses of various duration and polarity can be generated without the need to physically modify the device. SPICE simulation was performed to verify the suggested configuration for pulse generation. In addition, a practical design based on the suggested configuration was developed and tested to confirm the ability to generate nanosecond pulses with various duration, high repetition rate, and alternating polarity or not. Relatively large rise and fall times of generated pulses are mainly due to the delayed rise times of MOSFETs. We measured a maximal repetition rate of 1.1 MHz, which compared to previous publications is 100-fold higher [20]. Theoretically, this rate could be even higher; however, with our analog delay unit where we need to wait for the integrator to return to

the initial state, we were unable to generate the shorter delay  $A$  (Fig. 3). Comparable repetition rates (tested up to 100 kHz) can be achieved by diode-opening-switch-based nanosecond pulse generators [27]. However, with such a generator, pulse duration is not variable.

There are a few ways of manufacturing microelectrodes for nanosecond pulses. One is to glue the electrodes on cover glass. In this case, a very homogeneous electric field can be achieved in the gap between the electrodes by using thick electrodes on the order of a gap distance or larger. However, in this case, the electric field intensity in the gap just above the cover glass where the cells seed depends on the thickness of glue layer [6]. The second way is to deposit gold film on the photoresist structure. Developers of such a chamber report a well-defined structure of the electrodes, the possible separation of the photoresist and cover glass in aqueous environments, and a fluorescence background from the photoresist [28]. Another way is to deposit electrodes directly on the cover glass. In this case, the electric field is homogeneous just above the cover glass. Nevertheless, thick electrodes with sharp edges are needed to achieve a well-defined and homogeneous electric field in upper layers. Developers of such electrodes have made 20- $\mu\text{m}$ -thick electrodes from nickel [29] and silver [30]. We have made similar electrodes but from more biocompatible material—gold. The edges of the electrodes are almost vertical in the gap, except for the base Cr/Au layer that goes beyond the vertical for up to 1.5  $\mu\text{m}$  (Fig. 6). On the other hand, we made only 5- $\mu\text{m}$ -thick electrodes; therefore, further development is needed to achieve a more homogeneous electric field in the gap where the cells seed.

In 2001, the first evidence emerged that with the use of high-voltage nanosecond pulses, the permeabilization of internal cellular membranes can be achieved without severe cell plasma membrane damage [11]. Large endocytic vacuoles were permeabilized with no apparent effect on the plasma membrane integrity [8]. Theoretical predictions showed that the membranes of the cell organelles can be affected more than the cell plasma membrane, under some specific conditions [13]. Recent studies, using patch-clamp and molecular dynamics simulation studies, revealed that the cell plasma membrane is also permeabilized when high-voltage nanosecond pulses are applied to cells [31]–[33].

Our aim was to demonstrate the permeabilization of the endocytotic vesicles in cultured cells. With a double staining (lucifer yellow for endocytotic vesicles and propidium iodide for cell plasma membrane integrity [34]), we were able to observe the permeabilization of endocytotic vesicles and also cell plasma membrane permeabilization at the same time. The B16 F1 mouse melanoma cells were exposed to high-voltage nanosecond pulses that were generated by our new nanosecond pulser. When cells were exposed to 20 pulses with the duration of 60 ns, field strength of 50 kV/cm, and repetition rate 1 kHz in a pulse train, the permeabilization of endocytotic vesicles was achieved. At the same time as lucifer yellow is released from endocytotic vesicles, the propidium iodide enters the cells. Hence, the cell plasma membrane is also permeabilized after applying 20 high-voltage nanosecond pulses. The temperature rise of the cell suspension in the gap of our electrodes during our

experiment was calculated as a “worst-case” scenario where all the energy of all pulses is transformed into heat in one moment without any heat dissipation

$$\begin{aligned} \Delta T &= \frac{\Delta W}{c_m m} = \frac{E^2 \sigma}{c_m \rho} \Delta t \\ &= \frac{(50 \text{ kV/cm})^2 \times 1.67 \text{ mS/cm}}{[4200 \text{ J/(kg} \cdot \text{K)}] \times 1 \text{ kg/dm}^3} 1.2 \mu\text{s} = 1.2 \text{ K} \quad (1) \end{aligned}$$

where  $\Delta T$  is the temperature rise (in kelvins),  $\Delta W$  is the energy of all pulses (in joules),  $c_m$  is the heat capacity of the cell suspension (in joules per kilogram per kelvin),  $m$  is the mass of cell suspension in the gap (in kilograms),  $E$  is the electric field intensity in the gap (in volts per meter),  $\sigma$  is the electrical conductivity of cell suspension (in siemens per meter), and  $\rho$  is the density of the cell suspension (in kilograms per cubic meter). The electric field intensity in the gap is assumed to be homogeneous, and the heat capacity and density of the cell suspension to be the same as water. Based on this estimated temperature rise of 1.2 K, we can conclude that such an increase of temperature cannot play a major role in the observed biological effects.

The new design of the pulse generator was built, verified, and also tested in experiments. The resulting flexibility and variability will allow further *in vitro* experiments to reveal the importance of the pulse repetition rate and pulse polarity on membrane permeabilization—both of the cell plasma membrane as well as of cell organelle membranes.

#### ACKNOWLEDGMENT

The authors thank F. X. Hart for his help in the paper.

#### REFERENCES

- [1] E. Neumann, S. Kakorin, and K. Toensing, “Fundamentals of electroporative delivery of drugs and genes,” *Bioelectrochem. Bioenerg.*, vol. 48, pp. 3–16, 1999.
- [2] M. J. Jaroszkeski, R. Gilbert, C. Nicolau, and R. Heller, “*In vivo* gene delivery by electroporation,” *Adv. Drug Del. Rev.*, vol. 35, pp. 131–137, 1999.
- [3] J. Teissié, M. Golzio, and M. P. Rols, “Mechanisms of cell membrane electroporation: A minireview of our present (lack of ?) knowledge,” *Biochim. Biophys. Acta*, vol. 1724, pp. 270–280, 2005.
- [4] M. Puc, S. Čorović, K. Flisar, M. Petkovšek, J. Nastran, and D. Miklavčič, “Techniques of signal generation required for electroporation. Survey of electroporation devices,” *Bioelectrochemistry*, vol. 64, pp. 113–124, 2004.
- [5] M. Behrend, A. Kuthi, X. Y. Gu, P. T. Vernier, L. Marcu, C. M. Craft, and M. A. Gundersen, “Pulse generators for pulsed electric field exposure of biological cells and tissues,” *IEEE Trans. Dielectr. Electr. Insul.*, vol. 10, no. 5, pp. 820–825, Oct. 2003.
- [6] J. F. Kolb, S. Kono, and K. H. Schoenbach, “Nanosecond pulsed electric field generators for the study of subcellular effects,” *Bioelectromagnetics*, vol. 27, no. 3, pp. 172–187, 2006.
- [7] A. D. Blumlein, “Improvements in or relating to apparatus for generating electrical impulses,” GB Patent 589 127, 1947.
- [8] P. W. Smith, *Transient Electronics: Pulsed Circuit Technology*. New York: Wiley, 2002.
- [9] G. M. Loubriel, F. J. Zutavern, A. G. Baca, H. P. Hjalmarson, T. A. Plut, W. D. Helgeson, M. W. O’Malley, M. H. Ruebush, and D. J. Brown, “Photoconductive semiconductor switches,” *IEEE Trans. Plasma Sci.*, vol. 25, no. 2, pp. 124–130, Apr. 1997.
- [10] A. V. Martinez and V. Aboites, “High-efficiency low-pressure Blumlein nitrogen laser,” *IEEE J. Quantum Electron.*, vol. 29, no. 8, pp. 2364–2370, Aug. 1993.
- [11] K. H. Schoenbach, S. J. Beebe, and E. S. Buescher, “Intracellular effect of ultrashort electrical pulses,” *J. Membr. Biol.*, vol. 22, pp. 440–448, 2001.
- [12] K. H. Schoenbach, B. Hargrave, R. P. Joshi, J. F. Kolb, R. Nuccitelli, C. Osgood, A. Pakhomov, M. Stacey, R. J. Swanson, J. A. White, S. Xiao, J. Zhang, S. J. Beebe, P. F. Blackmore, and E. S. Buescher, “Bioelectric effects of intense nanosecond pulses,” *IEEE Trans. Dielectr. Electr.*, vol. 14, no. 5, pp. 1088–1109, Oct. 2007.
- [13] T. Kotnik and D. Miklavčič, “Theoretical evaluation of voltage induction on internal membranes of biological cells exposed to electric fields,” *Biophys. J.*, vol. 90, no. 2, pp. 480–491, 2006.
- [14] E. Tekle, H. Oubrahim, S. M. Dzekunov, J. F. Kolb, K. H. Schoenbach, and P. B. Chock, “Selective field effects on intracellular vacuoles and vesicle membranes with nanosecond electric pulses,” *Biophys. J.*, vol. 89, no. 1, pp. 274–284, 2005.
- [15] A. G. Pakhomov, R. Shevin, J. A. White, J. F. Kolb, O. N. Pakhomova, R. P. Joshi, and K. H. Schoenbach, “Membrane permeabilization and cell damage by ultrashort electric field shocks,” *Arch. Biochem. Biophys.*, vol. 465, no. 1, pp. 109–118, 2007.
- [16] P. T. Vernier and M. J. Ziegler, “Nanosecond field alignment of head group and water dipoles in electroporating phospholipid bilayers,” *J. Phys. Chem. B*, vol. 111, pp. 12993–12996, 2007.
- [17] S. J. Beebe, P. M. Fox, L. J. Rec, K. Somers, R. H. Stark, and K. H. Schoenbach, “Nanosecond pulsed electric field (nsPEF) effects on cells and tissues: Apoptosis induction and tumor growth inhibition,” *IEEE Trans. Plasma Sci.*, vol. 30, no. 1, pp. 286–292, Feb. 2002.
- [18] R. Nuccitelli, U. Pliquett, X. Chen, W. Ford, R. J. Swanson, S. J. Beebe, J. F. Kolb, and K. H. Schoenbach, “Nanosecond pulsed electric fields cause melanomas to self-destruct,” *Biochem. Biophys. Res. Commun.*, vol. 343, pp. 351–360, 2006.
- [19] E. B. Garon, D. Sawcer, P. T. Vernier, T. Tang, Y. Sun, L. Marcu, M. A. Gundersen, and H. P. Koeffler, “*In vitro* and *in vivo* evaluation and a case report of intense nanosecond pulsed electric field as a local therapy for human malignancies,” *Int. J. Cancer*, vol. 121, pp. 675–682, 2007.
- [20] P. T. Vernier, Y. Sun, and M. A. Gundersen, “Nanosecond-pulse-driven membrane perturbation and small molecule permeabilization,” *BMC Cell Biol.*, vol. 7, no. 37, pp. 1–16, 2006.
- [21] A. De Angelis, L. Zeni, and G. Leone, “Blumlein configuration for variable length high-voltage pulse generation by simultaneous switch control,” *Electron. Lett.*, vol. 42, no. 4, pp. 205–207, 2006.
- [22] A. De Angelis, J. F. Kolb, L. Zeni, and K. H. Schoenbach, “Kilovolt Blumlein pulse generator with variable pulse duration and polarity,” *Rev. Sci. Instrum.*, vol. 79, no. 4, pp. 1–4, 2008.
- [23] G. Pucihar, L. M. Mir, and D. Miklavčič, “The effect of pulse repetition frequency on the uptake into electroporated cells *in vitro* with possible applications in electrochemotherapy,” *Bioelectrochemistry*, vol. 57, pp. 167–172, 2002.
- [24] C. Blangero and J. Teissie, “Ionic modulation of electrically induced fusion of mammalian-cells,” *J. Membr. Biol.*, vol. 86, pp. 247–253, 1985.
- [25] G. Pucihar, T. Kotnik, M. Kanduđer, and D. Miklavčič, “The influence of medium conductivity on electroporation and survival of cells *in vitro*,” *Bioelectrochemistry*, vol. 54, pp. 107–115, 2001.
- [26] G. Pucihar, T. Kotnik, J. Teissie, and D. Miklavčič, “Electroporation of dense cell suspensions,” *Eur. Biophys. J.*, vol. 36, pp. 173–185, 2007.
- [27] A. Kuthi, P. Gabrielsson, M. R. Behrend, P. T. Vernier, and M. A. Gundersen, “Nanosecond pulse generator using fast recovery diodes for cell electromanipulation,” *IEEE Trans. Plasma Sci.*, vol. 33, no. 4, pp. 1192–1197, Aug. 2005.
- [28] Y. Sun, P. T. Vernier, M. Behrend, L. Marcu, and M. A. Gundersen, “Electrode microchamber for noninvasive perturbation of mammalian cells with nanosecond pulsed electric fields,” *IEEE Trans. Nanobiosci.*, vol. 4, no. 4, pp. 277–283, Dec. 2005.
- [29] S. M. Kennedy, Z. Ji, J. C. Hedstrom, J. H. Booske, and S. C. Haggness, “Quantification of electroporative uptake kinetics and electric field heterogeneity effects in cells,” *Biophys. J.*, vol. 94, pp. 5018–5027, 2008.
- [30] S. Katsuki, N. Nomura, H. Koga, H. Akiyama, I. Uchida, and S. I. Abe, “Biological effects of narrow band pulsed electric fields,” *IEEE Trans. Dielectr. Electr. Insul.*, vol. 14, no. 3, pp. 663–668, Jun. 2007.
- [31] A. G. Pakhomov, J. F. Kolb, J. A. White, R. P. Joshi, S. Xiao, and K. H. Schoenbach, “Long-lasting plasma membrane permeabilization in mammalian cells by nanosecond pulsed electric field (nsPEF),” *Bioelectromagnetics*, vol. 28, no. 8, pp. 655–663, 2007.
- [32] P. T. Vernier and M. J. Ziegler, “Nanosecond field alignment of head group and water dipoles in electroporating phospholipid bilayers,” *J. Phys. Chem. B*, vol. 111, no. 45, pp. 12993–12996, 2007.

- [33] B. L. Ibey, S. Xiao, K. H. Schoenbach, M. R. Murphy, and A. G. Pakhomov, "Plasma membrane permeabilization by 60- and 600-ns electric pulses is determined by the absorbed dose," *Bioelectromagnetics*, vol. 30, no. 2, pp. 92–99, 2009.
- [34] M. P. Rols, C. Delteil, M. Golzio, P. Dumond, S. Cros, and J. Teissié, "In vivo electrically mediated protein and gene transfer in murine melanoma," *Nature Biotechnol.*, vol. 16, no. 2, pp. 168–171, 1998.



**Matej Reberšek** was born in Ljubljana, Slovenia, in 1979. He received the Ph.D. degree in electrical engineering from the University of Ljubljana, Ljubljana.

He is currently a Research Associate in the Laboratory of Biocybernetics, Faculty of Electrical Engineering, University of Ljubljana. His current research interests include electroporation, especially design of electroporation devices and investigation of biological responses to nanosecond electrical pulses.



**Matej Kranjc** was born in 1983. He received the B.Sc. degree in electrical engineering from the University of Ljubljana, Ljubljana, Slovenia, where he is currently working toward the Ph.D. degree in electrical engineering at the Faculty of Electrical Engineering.

He is currently a Young Researcher in the Faculty of Electrical Engineering, University of Ljubljana. His current research interests include hardware development and numerical modeling of induction heating.



**Denis Pavliha** was born in Sempeter pri Gorici, Slovenia, in 1985.

Since 2005, he has been a demonstrator for undergraduate lectures on Computer Programming for Engineers I and II at the University of Ljubljana, Ljubljana, Slovenia, where he is currently an Undergraduate Student of electronics in the Faculty of Electrical Engineering, and joined the Laboratory of Biocybernetics in 2006, where he has been a Student Researcher in the field of electronics in biomedical engineering.

Mr. Pavliha received the Preseren Award by the Faculty of Electrical Engineering in 2008 for his work "controlling a nanosecond high-voltage generator for cell electroporation by a graphical user interface on an embedded computer."



**Tina Batista-Napotnik** was born in Ljubljana, Slovenia, in 1972. She received the B.Sc. degree in biology and the Ph.D. degree in medical sciences from the University of Ljubljana, Ljubljana.

She is currently a Research Associate in the Laboratory of Biocybernetics, Faculty of Electrical Engineering, University of Ljubljana. Her current research interests include electroporation, especially *in vitro* experimentation and investigation of biological responses to nanosecond electrical pulses.

**Danilo Vrtačnik** received the B.Sc., M.Sc., and Ph.D. degrees from the University of Ljubljana, Ljubljana, Slovenia, in 1981, 1994, and 2000, respectively.

Since 1991, he has been engaged in research on design, processing, and characterization of semiconductor devices in the Laboratory of Microsensor Structures and the Faculty of Electrical Engineering, University of Ljubljana, where he has been a Senior Researching Associate since 2007. During 1995, he was a Visiting Researcher at the Instituto per la Ricerca Scientifica e Tecnologica (IRST), Trento, Italy. His current research interests include development of silicon radiation detectors and related photodevices as well as advanced sensors and actuator structures fabricated by microelectromechanical systems (MEMS) technologies. He is included in numerous international and national projects and networks in the field of MEMS research and development. He is a reviewer for scientific journals and projects.

Dr. Vrtačnik is an Organizer and was the Chairperson of the International Conference on Microelectronics, Devices and Materials (MIDEM).



**Slavko Amon (M'75)** was born in Ljubljana, Slovenia, in 1945. He received the B.S. degree in physics from the Faculty of Natural Sciences and Technology, University of Ljubljana, Ljubljana, in 1970, and the M.S. and Ph.D. degrees in electrical engineering from the Faculty of Electrical Engineering, University of Ljubljana, in 1976 and 1981, respectively.

In 1970, he joined the Laboratory of Microelectronics, Faculty of Electrical Engineering, University of Ljubljana, where he was a Research Engineer in the field of planar silicon technology and devices, an Assistant from 1973 to 1982, was appointed as an Assistant Professor in 1982, an Associate Professor in 1987, and a Full Professor in 1992, giving courses in fundamentals of semiconductor devices, electron components, sensors and actuators, and established the Laboratory of Microsensor Structures in 1998. In 1978, he was on a six-month research visit at the Laboratoire de Microelectronique, Universite Catholique de Louvain, Louvain-La-Neuve, Belgium, as a "Chercheur libre," and worked on new MOS technologies. During 1992–1993 and 1994–1995, he was a Visiting Professor at Trento University, Italy, teaching and doing research in the modeling of semiconductor devices. His current research interests include micro-/nanomicroelectromechanical systems (nano-MEMS) structures and technologies, micromachining, modeling, and new microsensor and microactuator structures. He was a reviewer for international journals.

Dr. Amon is a member and currently the President of the International Microelectronics, Devices and Materials (MIDEM) Society. He is also a member of the Electrochemical Society. He was the Chairmen of the MIDEM International Conference. He was a member of the technical committees of several international conferences. He is currently a representative for Slovenia in European Nanoelectronics Initiative Advisory Council (ENIAC).



**Damijan Miklavčič** was born in Ljubljana, Slovenia, in 1963. He received the Ph.D. degree in electrical engineering from the University of Ljubljana, Ljubljana.

He is currently a Professor in the Faculty of Electrical Engineering, University of Ljubljana, where he is also the Head of the Laboratory of Biocybernetics. He is involved in the field of biomedical engineering. His current research interests include electroporation-assisted drug and gene delivery, including cancer treatment by means of electrochemotherapy, tissue

oxygenation, and modeling.